Evaluation of Transformation Expansion and Its Beneficial Effect on Cold Crack Susceptibility Using y-Slit Crack Test Instrumend with Strain Gauge†

Fukuhisa MATSUDA*, Hiroji NAKAGAWA**, Kenji SHINOZAKI*** and Hiroshi KIHARA****

Abstract

A new technique named "the Instrumented y-Slit Crack Test" was invented in order to estimate easily the effect of transformation expansion on the restraint stress using conventional y-slit crack test specimen utilizing strain gauges. Moreover, the effect of transformation expansion on cold cracking susceptibility is quantitatively investigated for SM41, SS41, HT60, HT80, HY130 and HY150 weldments by GTA and SMA weldings.

Consequently, the progress of contraction or restraint stress in the Instrumented y-Slit Crack Test can be estimated using this technique which is enough sensitive and good reproducibility. Therefore, this technique may be substituted for the RRC test in order to evaluate the effect of transformation expansion on cold cracking susceptibility.

For example in this study, the cracking ratio of HY150 weldment is much less than that of HT80 weldment in the y-slit crack test, and this new technique clearly revealed that this reason is owing to the reduction of restraint stress due to transformation expansion.

KEY WORDS: (Cold Cracking) (Transformation) (High Strength) (GTA Welding) (SMA Welding) (Restraint)

1. Introduction

For recent several years, the authors have studied the cause and the prevention method for high susceptibility to cold cracking of HY-type steel including mainly HY130 and partly HY150[1]. These series of studies[2),3] have shown that cold cracking susceptibility in weld metal of these HY steels is severer than in HAZ and the susceptibility evaluated with the LB-TRC test generally increases with an increase in strength level of base steel. On the other hand, the study[1),4] utilizing the RRC test has also revealed that restraint stress decreases with an increase in strength level due to phase transformation of weld zone from austenite to martensite. This may give a hope that cold cracking will be practically prevented by the aid of phase transformation in ultra high strength steels like HY-type steel. Therefore it may be important to reveal quantitatively the effect of transformation expansion on the cold cracking susceptibility.

However, the execution of the RRC test is very difficult in operation, although not so well known. Thus it may be very troublesome to evaluate the effect of transformation expansion by means of the RRC test, when optimum chemical composition in steel should be searched for the purpose of developing a new type of high strength steel.

By the way, many welding fabricators in Japan have usually used Tekken or the y-slit crack test to evaluate the welding and preheating conditions for the purpose of elimination of cold cracking. Judging from the shape of the y-slit crack test specimen, the specimen has two side restraint plates parallel to the weld line which the authors called "Side beam", and thus expansion and contraction of weld zone produce deformation of these two side beams. This gives an idea that the evaluation of expansion and contraction including the effect of transformation of weld zone may be possible in this test by measuring the deformation of side beams.

In this study, the new technique by which the deformation of side beams are evaluated utilizing strain gauges in the y-slit crack test has been developed. Then the authors have discussed the feasibility, applicability of this technique, and the correspondence between this technique and the RRC test. Moreover, the effect of transformation expansion on cold cracking susceptibility has been discussed in this test.

2. Principle of the Instrumented y-Slit Crack Test

This new technique is named "the Instrumented y-Slit Crack Test" by the authors which is instrumented with strain gauges on the y-slit crack test specimen, and

† Received on April 30, 1984
* Professor
** Research Instructor
*** Research Associate, Fuculty of Engineering, Osaka University
**** Emeritus Professor of Tokyo and Osaka Universities

Transactions of JWRI is published by Welding Research Institute of Osaka University, Ibaraki, Osaka 567, Japan

the principle is shown in **Fig. 1**. Four strain gauges ϵ_1, ϵ_2, ϵ_3 and ϵ_4 are stuck on each flank of the two side beams, among which ϵ_1 and ϵ_2 are active gauges and ϵ_3 and ϵ_4 are dummy gauges compensating thermal expansion of strain gauge for the purpose of increasing measurement accuracy. Now, supposing weld zone contracts and undergoes tensile stress, the flank of the side beam deform like the broken curve in Fig. 1, and thus the strain gauges should give a compressive value. Supposing weld zone expands and undergoes compressive stress, the flank of the side beam should deform like the dot-dash curve, and thus the strain gauges should give a tensile value. Therefore it should be roughly said that contraction and expansion of weld zone correspond to the compression and tension of the flank of side beam.

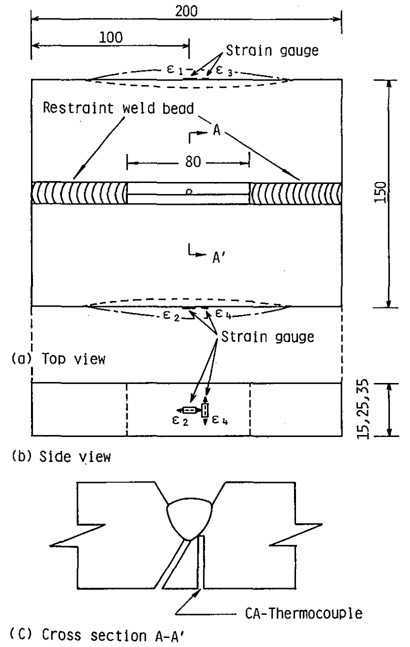

$\varepsilon^* = \varepsilon_1 + \varepsilon_2 - (\varepsilon_3 + \varepsilon_4)$
$= (1+\nu)(\varepsilon_1 + \varepsilon_2)$
$= 2(1+\nu)\varepsilon$
$\varepsilon = \varepsilon^* / 2.6$

ε: Strain on a flank
ε^*: Totally measured strain
ν: Poisson's ratio (=0.3)

Fig. 1 Configuration of the Instrumented y-Slit Crack Test specimen

Satoh et al. showed[4] that the contraction progress between two reference points of a welded joint where the weld length was very short was schematically illustrated like curve $\overline{OABCD}$ as shown in **Fig. 2 (a)**. In the first step from O to A, expansion occurs a little because of thermal expansion during welding. In the second step from A to B, contraction occurs because of homogenizing of temperature distribution toward thickness direction. In the third step from B to C, contraction is kept nearly constant because of limited temperature distribution inside of reference points. In the fourth step from C to D, contraction again occurs and progresses up to an inherent value given by heat input etc. because of diffusion of heat outward two reference points. Theoretically, when the gauge length is shorter, curve $\overline{OABCD}$ shifts to $\overline{OABC'D'}$. When the expansion of transformation from austenite to martensite in weld zone is effective, curve $\overline{OABCD}$ will shift to $\overline{OABC''D''}$. In the RRC test, the restraint stress is originated by applying reaction force against this contraction of weld zone.

There are of course some differences between the RRC test and the y-slit crack test. For example, (i) the y-slit crack test is not so rigid as the RRC test. (ii) Heat flow in the RRC test is generally one dimensional, but that in the y-slit crack test is two dimensional because of heat transfer to the restraint-welded parts. (iii) There are enough heat sink outside the reference points giving gauge length in the RRC test. However the restraint-welded parts described in (ii) gives large heat sink in the y-slit crack test.

The difference in (ii) and (iii) should give the next effects on the strain measurement discussed in this study; (a) the third step from B to C is not clear, (b) the fourth

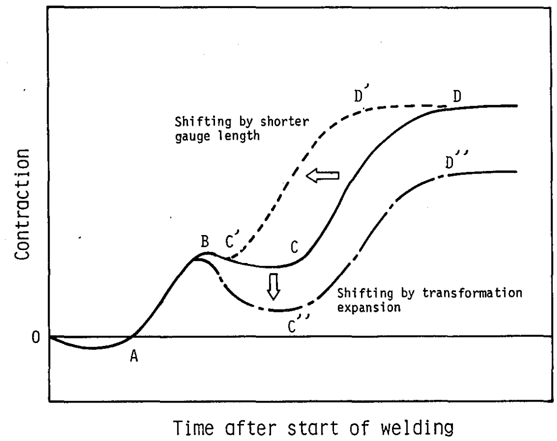

(a) Contraction progress

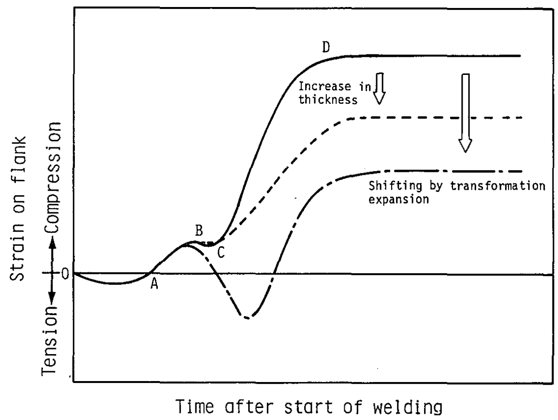

(b) Strain progress on a flank

Fig. 2 Contraction progress between (a) two reference points of a welded joint during and after welding obtained by Satoh et al. and (b) strain progress on a flank in the Instrumented y-Slit Crack Test step from C to D starts from earlier time, and the gradient is steeper. Although there are such differences discussed now, it is considered that the general tendency of the strain progress on the flank of a side beam in the Instrumented y-Slit Crack Test resembles the contraction progress in **Fig. 2 (a)**. Besides, it is guessed that the strain on the flank of the specimen decreases with an increase in thickness because deformation of the side beams become difficult.

These consideration schematically gives illustration as show in **Fig. 2 (b)**.

3. Materials Used and Experimental Procedure

3.1 Materials used

Base metals used were mild steels SM41*) and SS41*), and weldable heat-treated high strength steels HT60**), HT80**), HY130 and HY150 whose nominal ultimate strengths were 40, 60, 80, 100 and 120 kgf/mm^2, respectively.

Filler wires used for automatical GTA welding were well matched with base metals in strength levels, and named temporally as F41, F60, F80, F(130), $F(130)_{15N}$ and F(150) according to its strength level. Among them F41, F60 and F80 were commercial filler wires and the others were experimental ones. The diameters of them were 1.6 mm.

Covered electrodes used were D4316*), D5816*), D8016*), E(130)M and $E(130)_{9N}$ which well matched SM41, HT60, HT80 and HY130 in strength levels, respectively.

Designations, type of chemical compositions, yield strengths and ultimate tensile strengths of materials used were shown in **Table 1**.

3.2 Procedure of the Instrumented y-Slit Crack Test

The configuration of the Instrumented y-Slit Crack Test was already shown in Fig. 1. The thickness was 15, 25 and 35 mm. It is already accepted[5] that the restraint intensity R_F (kgf/mm·mm) is 70 times to the thickness (mm). Therefore the thickness of 15, 25 and 35 mm give the restraint intensity of 1050, 1750 and 2450kgf/mm·mm, respectively.

The strain measured in Fig. 1 was total value of four strain gauges. In this paper, the total strain was changed into the strain on one flank of the specimen parallel to the weld line using the equation as shown in Fig. 1.

Weld bead was laid in the y-groove with root gap of 2 mm by GTA or SMA welding without any treatments of arc start and finish. The GTA and SMA welding conditions used were welding current of 300A and 170A, arc voltage of 14 V and 25 V, and welding speed of 120 mm/min and 150 mm/min, respectively. Preheating temperature were 50°C for GTA welding, and 50 and 75°C for SMA welding. Any grease of filler wire was cleaned out by acetone and covered electrodes were dried at baking temperature of 400°C for 1 hour before welding. Diffusible hydrogen content was measured by means of gas chromatograph whose measurement accuracy was 0.01 ml. Diffusible hydrogen contents of deposited metals used were shown in **Table 2**.

Table 2 Diffusible hydrogen content in deposited metal by SMA and GTA weldings

Materials		Diffusible hydrogen content (ml/100g)
Covered electrode (SMAW)	D4316	7.0
	D5816	3.3
	D8016	2.2
	E(130)M	2.2
	$E(130)_{9N}$	1.6
Filler wire (GTAW)	F41	0.4
	F60	0.2
	F(130)	0.2
	$F(130)_{15N}$	0.2
	F(150)	0.2

Table 1 Designation, type of chemical compositions, yield and tensile strengths of materials used

Base metal [15,25,35 mm thickness]	Covered electrode [4 mm dia.]	Filler wire [1.6 mm dia.]	Yield strength of base metal (kgf/mm^2)	Ultimate strength of base metal (kgf/mm^2)
SM41, SS41	D4316	F41	22	45
HT60 (0.1Mo-V)	D5816 (0.6Ni)	F60 (0.4Mo)	55	65
HT80 (1.3Ni-Cr-Mo-V)	D8016 (1.7Ni-Cr-Mo)	-	78	84
HY130 (5.1Ni-Cr-Mo-V)	E(130)M (2.7Ni-Cr-Mo) $E(130)_{9N}$ (8.7Ni-Cr-Mo)	F(130) (2.5Ni-Cr-Mo) $F(130)_{15N}$ (15Ni-Cr-Mo)	96	102
HY150 (8.6Ni-Cr-Mo-V)	-	F(150) (8.3Ni-Cr-Mo)	115	120

*) These designations follow JIS (Japan Industrial Standard)
**) Common name in Japan

4. Experimental Result and Discussion

4.1 Behavior of contraction and expansion

Figures 3 (a) and **(b)** show the progress of strain on the flank of side beam in different combinations of base metals and filler wires with the cooling curve in the middle of weld bead in the thickness of 15 and 35 mm. Plus or minus side in the ordinate indicates the compressive or tensile strain, respectively. Generally, residual tensile strain or compressive strain corresponds to the residual tensile stress or compressive stress in weldment, but the compressive strain or tensile strain on the flank corresponds to the tensile stress or compressive stress in this test.

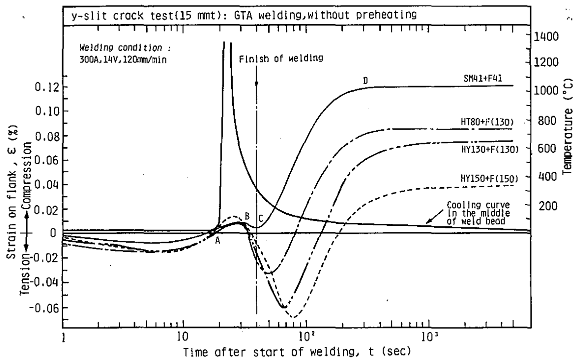

(a) 15 mm thickness

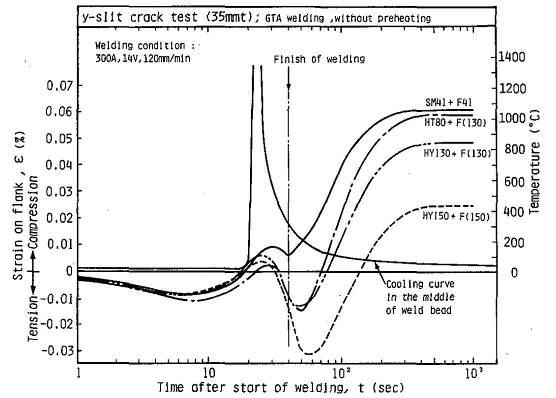

(b) 35 mm thickness

Fig. 3 Progress of strain on a flank in SM41, HT80, HY130 and HY150 weldments of both thicknesses of 15 and 35 mm

Now, compared the progress of contraction in shorter gauge length, namely curve $\overline{OABC'D'}$ in Fig. 2 with that of strain in SM41 in Fig. 3, both behaviors have a resemblance to each other. Namely, in Fig. 3 (a) for example, tensile strain occurs for 20 sec after start of welding (O-A: corresponding to the first step), and then continuously changes to compressive strain for 10 sec (A-B: corresponding to the second step). Then the compressive strain slightly decreases for 10 sec (B-C: corresponding to the third step) and again increases gradually to the final value of about 0.12% (C-D: corresponding to the fourth step). The final value of the strain was named the maximum strain, ϵ_m.

In Fig. 3 (a), the progress of strain in HT80, HY130 and HY150 weldments are different from that in SM41. For example, the tensile strain in HT80 approximately agrees with that in SM41 in the range of O to A and continuously changes to the compressive strain after start of welding. However, this compressive strain rapidly decreases before reaching B in SM41, then again change to the tensile strain. This tensile strain increases for 20 sec and again gradually decreases and changes to the compressive strain. Then this compressive strain gradually increases to the final value of about 0.08% in the time period from 50 to 500 sec after start of welding. The progress of strain in HY130 and HY150 weldment show similar mode to that in HT80 weldment, and ϵ_m decreases in the order of SM41, HT80, HY130 and HY150 weldment. The mode of the progress of strain in the thickness of 35 mm shown in Fig. 3 (b) is similar to that in the thickness of 15 mm shown in Fig. 3 (a), though each ϵ_m is lower in Fig. 3 (b) than in Fig. 3 (a). Moreover, the difference in ϵ_m between SM41 and HT80 weldments is very small owing to yielding in SM41 in Fig. 3 (b).

It is noteworthy that ϵ_m decrease in the order of SM41, HT80, HY130 and HY150 weldment. Then, the relationship between temperature in the middle of weld bead and the strain is shown for 35 mm thickness specimen in **Fig. 4** for the purpose of understanding the reason why the strains in HT80, HY130 and HY150 weldment especially decrease in the third and fourth steps. In this figure, the compressive strains in HT80, HY130 and HY150 decrease and change to the tensile strains in the temperature range approximately corresponds to the M_s temperature in base metal and weld metal as shown in the previous report[1] using the dilatometric technique, that is, 410 – 450°C for HT80, 370 – 400°C for HY130 and 300 – 310°C for HY150 weldment.

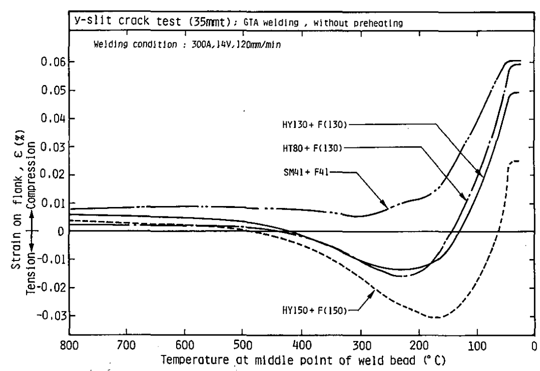

Fig. 4 Relationship between temperature at middle point of weld bead and the strain on a flank

Judging from the above mentioned, the decrease in the compressive strain in HT80, HY130 and HY150 weldments except for SM41 weldment in the third and fourth steps is strongly related to the expansion of transformation from austenite to martensite. It seems that transformation expansion doesn't effectively influence to SM41, because transformation temperature is so high that plastic deformation easily occurs in weld zone. Moreover, the progresses of the strain on the flank in HT80, HY130 and HY150 weldments in Fig. 3 roughly correspond to that of the restraint stress shown in **Fig. 5** obtained in the previous report[1]. The reason why the time when the restraint stress rapidly increases from zero is longer in the RRC test than the time when compressive strain rapidly increases from zero in this study is considered to be due to the difference in (ii) as described in section 2.

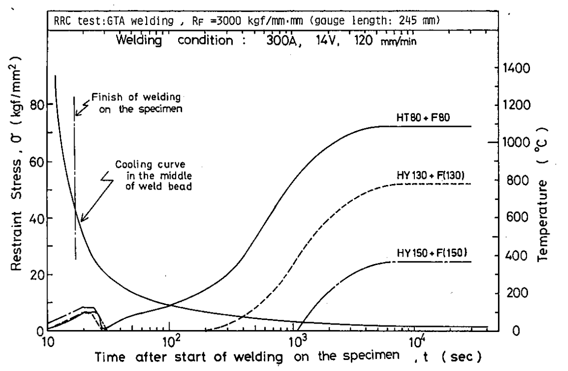

Fig. 5 Progress of the restraint stress in the RRC test of the restraint intensity of 3000 kgf/mm·mm obtained in the previous paper[1]

Figure 6 shows the progress of strain in cracked weldment. In this case, also acoustic emission technique was used, and gave a information that crack surely occurred at about at latest 10^3 or 10^4 sec in Fig. 6. Moreover, naked eye could detect surface crack when the strain gradually reduced in Fig. 6. Therefore these mean that the strain was kept nearly constant even after the crack occurrence to some extent, and then gradually decreases at the late period of the fourth step because of the remarkable crack propagation. Therefore it is difficult by this technique to detect the term of crack initiation. **Figure 7** schematically illustrates the progress of strain in the case of both cracked and crack-free weldments. It may be considered that ϵ'_m in cracked weldment is lower than ϵ_m in crack-free weldment. However cracking seldom affected practically ϵ_m, because there is no difference in ϵ_m between cracked and crack-free weldment as later shown in Fig. 13.

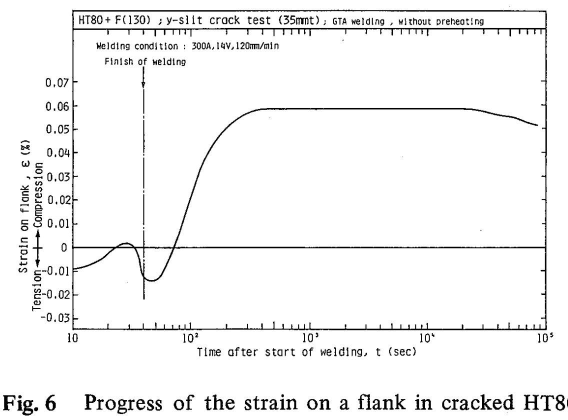

Fig. 6 Progress of the strain on a flank in cracked HT80 weldment

Consequently, measurement of the strain on the flank of a side beam is very available to estimate simply the effect of transformation expansion on the contraction in weld zone. Moreover, it seems that ϵ_m in the Instrumented y-Slit Crack Test is as important as the final restraint stress in the RRC test for estimating cold cracking susceptibility. Therefore, ϵ_m is mainly discussed hereafter.

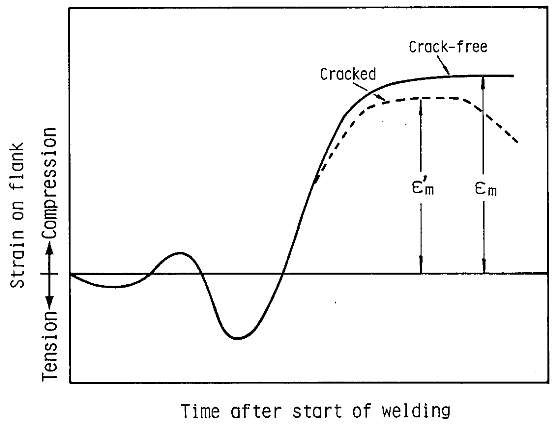

Fig. 7 Schematic illustration of the strain progress on a flank in crack-free and cracked weldments in principle (ϵ'_m is actually equal to ϵ_m)

4.2 Study on the maximum strain

4.2.1 Correlation between the restraint intensity and the maximum strain

Figure 8 shows the relationship between the restraint intensity (R_F) and ϵ_m, where ϵ_m decreases with an increase in strength level of materials used, namely in the order of SM41, HT80, HY130 and HY150 due to the effect of transformation expansion. Moreover, ϵ_m in each weldment except for SM41 decreases approximately proportional to R_F in the range about 1000 to 2500 kgf/mm·mm. As already decribed, the reason why there is no difference in ϵ_m between SM41 and HT80 weldment in R_F of 2450 kgf/mm·mm is considered to be due to yielding of SM41 weldment. Each gradient of these lines approximately decreases with an increase in strength level. The reason why increase in strength level or restraint intensity decreases ϵ_m was already described in section 2.

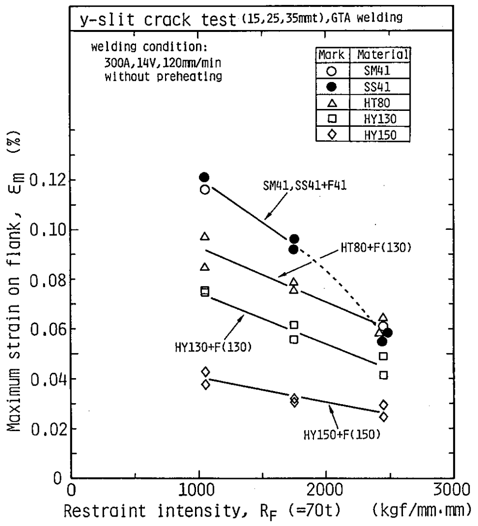

Fig. 8 Relationship between the restraint intensity and the maximum strain on a flank

4.2.2 Correlation between transformation expansion and the maximum strain

As already shown, the transformation expansion influences ϵ_m. The authors have shown in the previous paper[1] that the relief of the restraint stress is owing to the transformation expansion of weld zone including weld metal and HAZ.

The relationship between the transformation expansion of weld zone (δ_t) measured in the previous paper[1] and ϵ_m is shown in **Fig. 9**, where ϵ_m in the thickness of 15 and 25 mm except for 35 mm decrease approximately linearly up to HY130 weldment and then drastically with the increase in δ_t. Also in the case of 35 mm thickness, generally decreasing tendency is observed except for an abnormal result for SM41 and SS41 which is attributed to yielding of weld zone as already mentioned. It is noteworthy that the correlations in the case of 15 and 25 mm thickness in Fig. 9 well resemble the correlation between δ_t and the final restraint stress in the RRC test of the previous report[1]. The reason why these correlations is not linear but very steep from HY130 to HY150 is considered to be the low transformation temperature of HY150 as already discussed in the previous report.

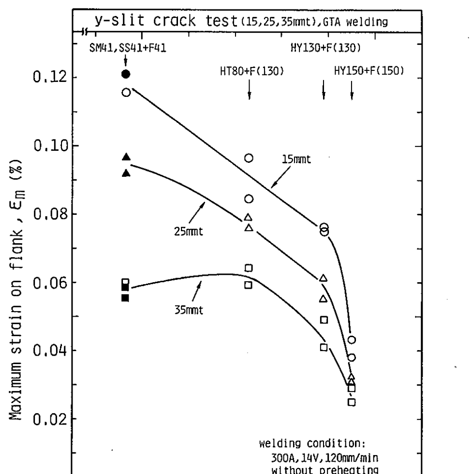

Fig. 9 Relationship between transformation expansion of weld zone and the maximum strain on a flank

4.3 Correlation between the maximum strain and the final restraint stress in the RRC test

The authors think that the RRC test is very instructive for understanding the reducing effect of the restraint stress due to transformation expansion, but is experimentally a little troublesome in operation. Therefore, it is very useful for the welding fabricators to know simply the effect of transformation expansion on the restraint stress by substituting the Instrumented y-Slit Crack Test for the RRC test. For this purpose, it is necessary to correlate ϵ_m with the final restraint stress in the RRC test ($(\sigma_\infty)_{RRC}$).

Then, the relationship between R_F and $(\sigma_\infty)_{RRC}$ in the previous report[1] was related to that between R_F and ϵ_m in Fig. 8. **Figure 10** shows the relationship between $(\sigma_\infty)_{RRC}$ and ϵ_m in the restraint intensities of 1050, 1750 and 2450 kgf/mm·mm. It is interesting that $(\sigma_\infty)_{RRC}$ increases approximately proportional to ϵ_m under each restraint intensity independently of materials used. Therefore, the ratio of $(\sigma_\infty)_{RRC}$ and ϵ_m, namely $(\sigma_\infty)_{RRC}/\epsilon_m$ is approximately decided by the restraint intensity independently of materials as shown in **Fig. 11.** Consequently, $(\sigma_\infty)_{RRC}$ can be practically estimated by measurement of ϵ_m in the Instrumented y-Slit Crack Test

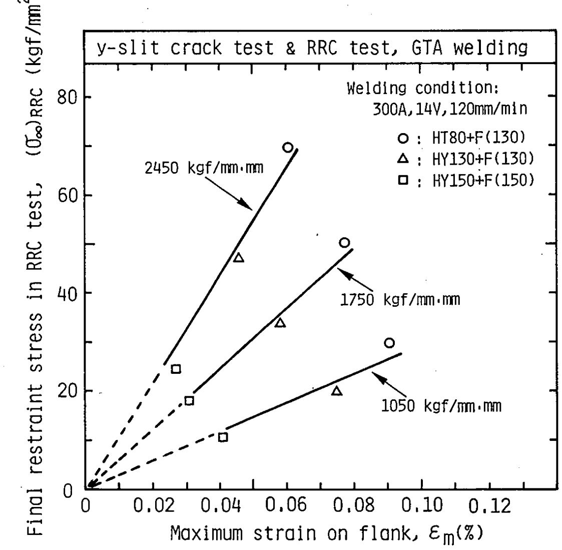

Fig. 10 Relationship between the maximum strain on a flank and the final restraint stress in the RRC test

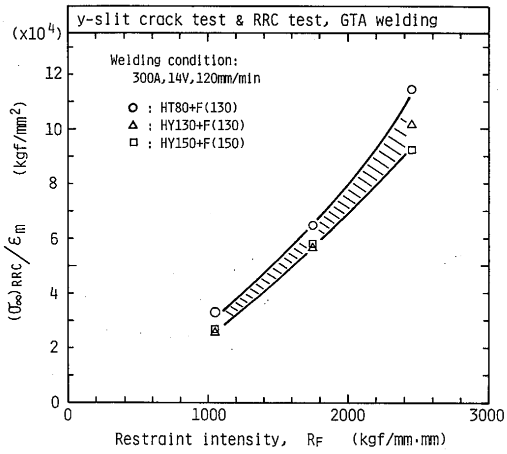

Fig. 11 Relationship between the restraint intensity and the value of $(\sigma_\infty)_{RRC}/\epsilon_m$

under the same restraint intensity. For example, supposing the restraint intensity is 2000 kgf/mm·mm and ϵ_m measured is 0.04% in the Instrumented y-Slit Crack Test, $(\sigma_\infty)_{RRC}/\epsilon_m$ gives about 7.7×10^4 according to Fig. 11. Therefore, $(\sigma_\infty)_{RRC}$ is estimated to 31 kgf/mm^2.

4.4 Effect of combination of base metal and weld metal on the maximum strain

Since the value of transformation expansions and transformation temperatures of base metal and weld metal are respectively different from each other, it is important to know the total effect of the combination of base metal and weld metal on ϵ_m.

Figures 12 (a) and **(b)** show ϵ_m in different combination of base metal of 35 mm thickness and welding rods by GTA and SMA weldings, respectively. In Fig. 12 (a) of GTA welding, ϵ_m generally decreases with an increase in strength level or alloying element of base metal or filler wire, namely in the order of HT60, HT80, HY130 and HY150 steels except for SM41 steel independently of preheating temperature. Similarly in Fig. 12 (b) of SMA welding, ϵ_m generally decreases in the same tendency. These results mean that both base metal and welding rod contribute the reducing of ϵ_m, namely the reducing of the final restraint stress in the y-slit crack test.

4.5 Effect of transformation expansion on cold cracking susceptibility

Figures 13 (a) and **(b)** show ϵ_m, hardness of weld metal and HAZ, and cracking ratio (C_a) in SM41, HT60, HT80, HY130 and HY150 weldments by GTA and SMA weldings using welding rods well matching base metal, respectively. As shown in previous reports[3], the lower critical stresses of HY130 and HY150 with the TRC test and the LB-TRC test are lower than that of HT60 or HT80

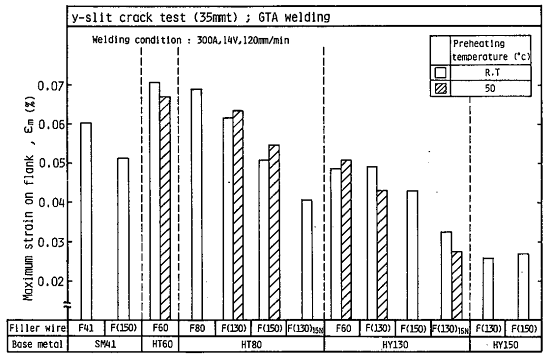

(a) GTA welding

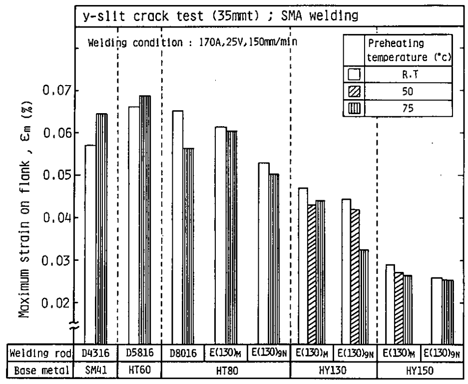

(b) SMA welding

Fig. 12 Effect of combination of base metal and weld metal on the maximum strain on a flank

weldment, so it is reasonable to expect that the cracking ratios of both HY130 and HY150 weldments are higher than that of HT60 or HT80 weldment. However in Fig. 13 (a) of GTA welding, the cracking ratios of HY130, HY150 and SM41 weldments are much lower than those of HT60 and HT80 weldments independently of preheating temperature. Especially, cracking ratio of HY150 weldment is zero even without preheating. Lower cracking ratio in SM41 weldment may be owing to lower hardness of weld metal. On the other hand, since hardness of weld zone and diffusible hydrogen contents shown in parentheses of materials except for SM41 weldment is almost constant, lower cracking ratio in HY130 or HY150 weldment may be owing to the lower restraint stress which corresponds to the lower ϵ_m. In Fig. 13 (b) of SMA welding, cracking ratios of SM41, HT60, HT80 and HY150 weldment in without preheating are about 85 to 95%, but that of HY150 weldment is about 10%. Moreover, cracking ratio of HY150 weldment is zero with preheating temperature of 50°C, and then those of HY130 and HT60 weldments except for SM41 are zero with preheating temperature of 75°C, but that of HT80 and SM41 weldments are about 100 and 40%, respectively. Higher susceptibility to cold cracking in this SM41 weldment is owing to higher diffusible hydrogen content in this case.

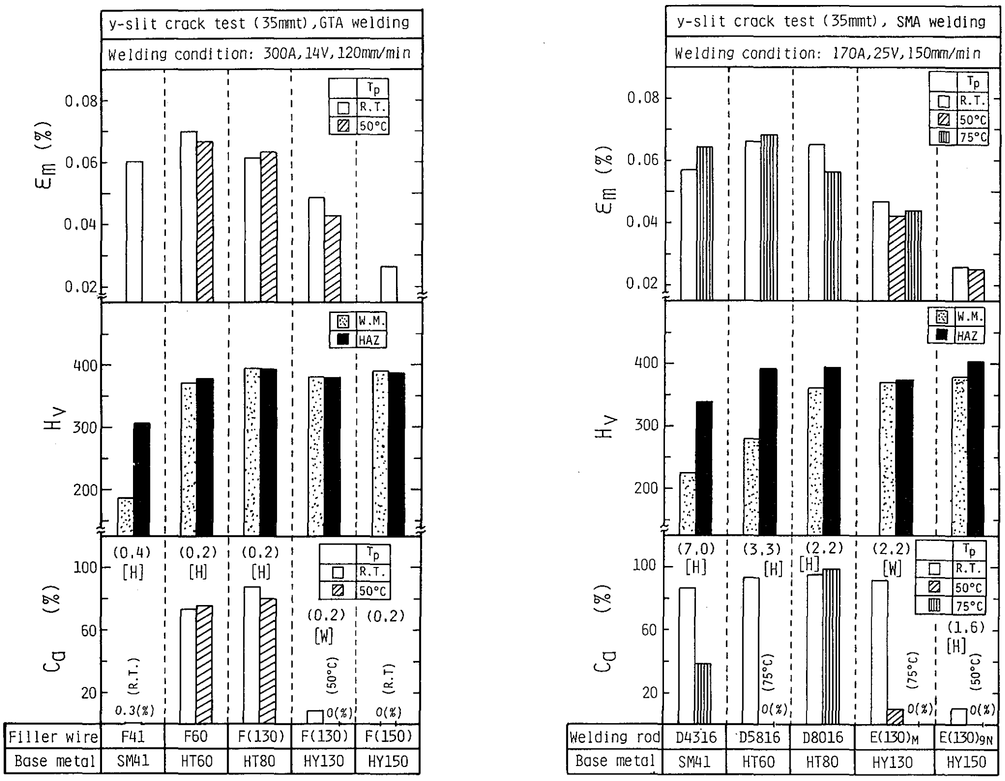

(a) GTA welding (b) SMA welding

Fig. 13 Effect of transformation expansion on cold cracking susceptibility

ϵ_m: Maximum strain on a flank
H_v: Vickers hardness number
C_a: Area fraction of fractured surface
T_p: Preheating temperature
( ): Diffusible hydrogen content (ml/100g)
[H] :Crack initiated in HAZ
[W] :Crack initiated in weld metal

On the other hand, the reason why cold cracking ratios of HY130 and HY150 are lower than that of HT80 weldment may be owing to the reducing of restraint stress as the same reason in Fig. 13 (a). Thus lower cracking susceptibility in HY130 and HY150 weldments are strongly affected by reducing the restraint stress due to transformation expansion.

Consequently, this study revealed that the evaluation of cold cracking susceptibility by the TRC test and perhaps by the Implant test in which constant load is applied is too severe for such steel as HY130 and HY150 because of their low restraint stress due to much effect of transformation expansion. Similarly, cold cracking parameter such as P_w[6] concept is not available for such steel as HY130 or HY150, because the parameter of the effect of transformation expansion is not included in P_w. As the future subject, it is necessary to establish a cold cracking parameter which includes not only the effects of hardenability, diffusible hydrogen content and restraint intensity but also the effect of transformation expansion.

5. Conclusion

A new technique named the Instrumented y-Slit Crack Test was invented in order to estimate easily the effect of transformation expansion on the restraint stress using convensional y-slit crack test specimen, and was also applied to evaluate the cracking ratio. Consequently, the effect of transformation expansion on cold cracking susceptibility studied in such steels as SM41, SS41, HT60, HT80, HY130 and HY150 by GTA and SMA weldings.

Main conclusions obtained are as follows;

(1) In the Instrumented y-Slit Crack Test, strain gauges are stuck on the flanks parallel to the weld line of the y-slit crack test specimen, and the progress of strain during and after welding is monitored. This technique is enough sensitive and gives good reproducibility.

(2) The behavior of strain progress by this technique resembles that of the restraint stress in the RRC test. Therefore, the effect of transformation expansion on the strain is clearly seen as the effect of transformation expansion on the restraint stress in the RRC test.

(3) Since the execution of the RRC test is generally a little difficult in operation, this technique can be substituted for the RRC test because this technique is very easy and useful to evaluate quantitatively the effect of transformation expansion on cold cracking suscep-

tibility. For example, the cracking ratio of HY150 weldment is much less than that of HT80 in the y-slit crack test, and this new technique clearly revealed that this reason is owing to the reduction of restraint stress due to transformation expansion.

Judging from the above, the completion of crack-free weldment may be practically obtainable in higher strength steels as HY-type steel using transformation expansion.

Acknowledgement

The authors would like to express our gratitude to Mr. Katsuyuki Harada, formerly student of Osaka Institute of Technology, for his cooperation of testing and to thank Nippon Steel Corporation and Mitsubishi Heavy Industries Corporation for offering materials used in this investigation.

References

1) F. Matsuda et al.: Trans. JWRI, Vol. 11 (1982), No.2, pp. 57–65.

2) F. Matsuda et al.: Trans. JWRI, Vol. 6 (1977), No.2, pp. 59–73.

3) F. Matsuda et al.: Trans. JWRI, Vol. 8 (1979), No.1, pp. 113–119.

4) K. Satoh et al.: Technical Reports of Osaka Univ., Vol. 17 (1967), No.783, pp. 353–375.

5) JSSC, Vol. 8 (1972), No.80, pp. 22–50 (in Japanese)

6) Itoh et al.: J. Japan Weld. Soc., Vol. 38 (1969), No.10, pp. 1134–1144.